

## MODELING OF QUANTUM BARRIER DEVICES USING QUANTUM MOMENT EQUATIONS

JING-RONG ZHOU and DAVID. K. FERRY  
*Center for Solid State Electronics Research  
 Arizona State University, Tempe, AZ 85287-6206*

### Abstract

We describe the numerical simulation of ultra-submicron high electron mobility transistors using a set of quantum moment equations. The simulation shows that a large change of electron density distribution arises from the inclusion of quantum corrections. The total current is increased by as much as ten per cent due to the quantum effects, mainly due to the softening of the gate depletion potential resulting in a higher electron density distribution along the channel. Tunneling effects do not give a noticeable contribution to the total current in the simulated device. To test the ability of the method for describing tunneling, simulation of a resonant tunneling diode with this set of equations is also discussed.

### Degeneracy in the Quantum Moment Equations

We have previously developed a set of quantum moment equations based upon the Wigner function equation-of-motion [1,2]. The first approach to explicit quantum corrections are built into these equations through the second moment of the Wigner function [3], which results in an average electron energy that consists of drift kinetic, thermal, and quantum potential (or pressure) terms. Application of these equations to the numerical simulation of ultra-submicron GaAs MESFETs demonstrated the expected quantum effects in the devices [3,4]. Here, we apply this model to study ultra-submicron quantum barrier devices, e.g. HEMT, with the investigation of quantum effects as the prime objective. As previously, the quantum pressure term serves to soften potential variations. This leads to a large change of the density distribution in the channel, with a consequent increase in the total current by more than ten per cent. Other than the quantum pressure term, described below, these equations are the same as used by others [5]. Here, however, we also include carrier degeneracy. Modifications can be made directly to the moment equations by assuming a drifted Fermi-Dirac distribution function [6], which is represented by a correction factor to the effective electron temperature. The total average electron kinetic energy can now be written as:

$$w = \frac{1}{2}m^*v^2 + \frac{3}{2}\gamma k_B T + U_q, \quad (1)$$

where  $U_q$  is the quantum pressure term,

$$U_q = -\frac{\hbar^2}{8m^*} \nabla^2 \ln(n), \quad (2)$$

and  $\gamma$  is the degeneracy factor,

$$\gamma = \gamma(\mu_f/k_B T) = \frac{F_{3/2}(\mu_f/k_B T)}{F_{1/2}(\mu_f/k_B T)}. \quad (3)$$

Here,  $F_j$  is the Fermi-Dirac integral, and  $\mu_f$  is the Fermi energy measured from the conduction band edge.

Because the Fermi energy is directly related to the electron density in the conduction band, its relation to the density and temperature can be expressed by a drifted Fermi-Dirac distribution function [6],

$$n = 2 \left( \frac{2\pi m^* k_B T}{h^2} \right)^{3/2} F_{1/2}(\mu_f / k_B T). \quad (4)$$

We do not need to evaluate the Fermi energy explicitly to get the value of the degeneracy factor  $\gamma$ , because the Fermi integration is actually determined by the ratio of the Fermi energy and the thermal energy, say  $\eta_f = \mu_f / k_B T$ . From this,

$$n / (k_B T)^{3/2} = \frac{4}{\pi^{1/2}} \left( \frac{2\pi m^*}{h^2} \right)^{3/2} F_{1/2}(\mu_f / k_B T). \quad (5)$$

With this expression, we can establish a relationship between the factor  $n / (k_B T)^{3/2}$  and the degeneracy  $\gamma$ . This relation can then be tabulated in the simulation program and the degeneracy factor handled easily once the density and temperature are computed from the moment equations. This process is done self-consistently, but could be approximated by using the values at the previous time step. Thus, the inclusion of the degeneracy effect into the moment equations does not increase the computational efforts.

Degeneracy may also introduce modifications to the velocity-field and energy-field characteristics [7,8], which in turn will introduce modifications to the relaxation times, as the momentum and energy relaxation times are computed from Monte Carlo results. However, if one assumes that the increase of the energy due to degeneracy is essentially the thermal energy  $3k_B \gamma T / 2$  [9], then the use of scattering rates from the Monte Carlo results without degeneracy, but calculated at  $T$  instead of  $\gamma T$ , remains a good approximation. We follow this approach.

### Simulation of HEMT Devices

For an ideal AlGaAs/GaAs interface, the transition of the conduction band from one material to another is abrupt. Electrons in the quantum well are prevented from drifting into the AlGaAs by the potential step (the band offset). Electrons can climb over the potential wall only if they have a kinetic energy comparable to the step barrier height. There is a problem in that the partial differential equations (primarily the moment equations) do not handle the band discontinuity, where an infinite field is met. While an abrupt change in the transition from one material to another may be ideal, there is a certain transition region to be expected [9]. In our simulation, we assume a 0.3 V potential drop across a 4 nm region at the interface. While this seems to be quite wide, it is a statistical average over the actual transition region and the wavefunction decay at this interface [10].

The doping is taken to be  $1.5 \times 10^{18} \text{ cm}^{-3}$  in the AlGaAs and  $1.0 \times 10^{14} \text{ cm}^{-3}$  in the GaAs. The AlGaAs layer thickness is 40 nm. The high doping density in the AlGaAs helps to confine the gate depletion to a size compatible to the gate length. With low doping, a wide potential barrier occurs [11]. The lattice temperature is taken to be 300 K. A detailed description of the numerical simulation can be found in [3]. The results discussed here are for a 24 nm gate length device.

The I-V characteristics for a 24 nm gate length HEMT device are shown in Fig. 1, where the gate bias runs from 0 volt to -2.5 volts, in steps of -0.5 volts. In Fig. 2, the electron density at the center of the gate is plotted as a function of the distance from the surface into the bulk at a bias condition of  $V_g = -1.5 \text{ V}$  and  $V_d = 1.0 \text{ V}$ . In this figure, we show the results with the quantum pressure included (solid line) and neglected (dashed line). It is clear that the quantum corrections change the interface potential. One can see that for the bias condition of Fig. 2, a parallel conduction channel in the AlGaAs is present.

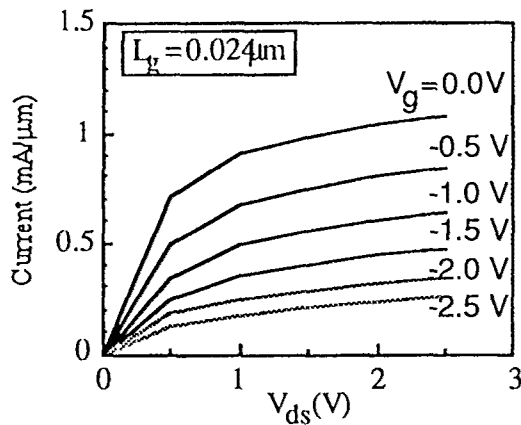


Fig. 1. I-V characteristics.

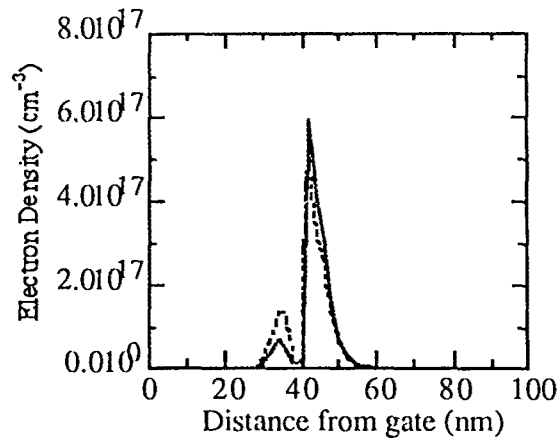


Fig. 2. Electron density distribution across the conduction channel as the function of distance to the gate contact.

The drain current is plotted in Fig. 3 for a gate bias of  $-1.5$  V. These results illustrate the various cases. The increase of the current with degeneracy included is expected, as the scattering rates are lowered because of the lack of empty states at the final state due to Pauli exclusion [7]. Degeneracy is prominent only close to the source where the effective electron temperature is low. Because the length scale of the device is small, electrons entering from the source contact will travel through the low-field region in a short time. Monte Carlo simulation of the time evolution of electron velocity predicts that the transient velocity is larger for a degenerate case on a short time scale (about 0.5 picosecond) as the field is turned on [8]. This also suggests that electrons will have higher velocity with degeneracy included, resulting in a higher drain current.

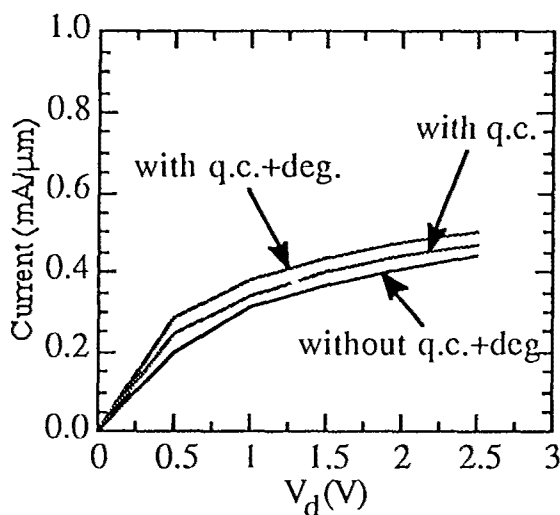


Fig. 3. Drain current characteristics for  $V_g = -1.5$  V.

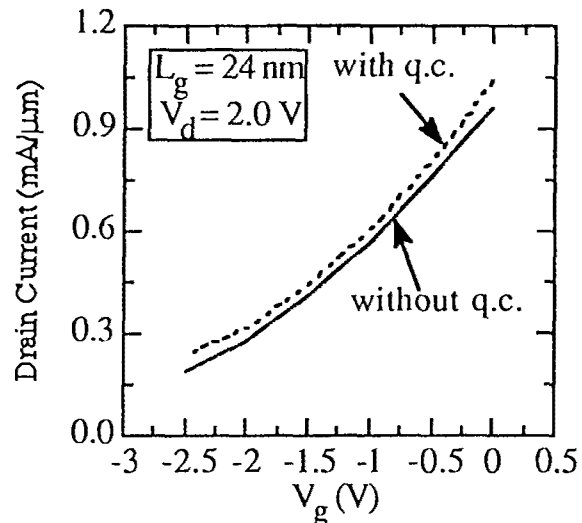


Fig. 4. Drain current characteristics at  $V_g = -1.5$  V.

The quantum corrections serve to smooth the classical potential, which in turn smooths the electron density distribution. As can be seen in Fig. 2, quantum corrections introduce a large change in the density distribution. The density peak is reduced in the AlGaAs and increased in the 2-D gas when the quantum corrections are included. In the AlGaAs the electron density distribution under the gate (along the channel) is relatively flat, when compared to the direction normal to the interface. The interface potential is broadened (towards the gate) and quantum

corrections along the channel direction are small, and these effects result in a lower density peak. Due to the high electron density in the 2-D gas, the quantum correction along the channel direction dominate, so the net effect is an increase of electron density, resulting in a fatter and higher peak. Quantum corrections make an appreciable change in the current distribution in the conduction channel as a result. This change is as much as 10 per cent increase in the total current with quantum effects included, and leads to the differences observed in Fig. 3.

The increase of the total current, especially the increase of the peak electron density in the channel, suggests tunneling processes (through the depletion region included by the gate) may occur in the device operation. However, there are two facts suggesting that the process should not be interpreted as tunneling. It is well known that the tunneling current should exponentially decrease with an increase of the potential barrier. Thus, one expects that quantum effects (such as tunneling) will become smaller as we increase the drain voltage or decrease (more negative) the gate voltage. The depletion barrier will be widened in both cases. This is not observed in our present simulation. The drain current is plotted against gate voltage in Fig. 4 for simulations with and without quantum corrections. As can be seen, the current increase due to quantum effects is relatively insensitive to the gate voltage. A similar property can be found in Fig. 3, in which the current increase due to quantum effects is relatively insensitive to the drain voltage. These results lead us to the conclusion that, if there is any tunneling, the tunneling current must be small.

### Simulation of Resonant Tunneling Diode

The resonant tunneling diode (RTD) is a good subject to test the ability of the quantum moment equations in describing the tunneling effect. The modeling method for the HEMT interface barrier may be readily extended to model the barriers of a RTD. For a double barrier RTD with the structure of GaAs/AlGaAs/GaAs/AlGaAs/GaAs, one can model the two barriers with four step barriers, each step barrier with a transition region of several angstroms. To simulate a barrier thickness of 5 nm or less, one may need the smallest grid size to be one or two angstroms. This will introduce a electrical field of  $10^6$  V/cm in the barrier transition regions. A suitable numerical scheme must be used to deal with these transition regions. We are currently working on this problem.

This work is supported by the Army Research Office. The authors thank Dr. Qin Li and T. Yamada for useful discussions.

### References

- [1] E. Wigner, *Phys. Rev.* **40**, 749 (1932).
- [2] G. J. Iafrate, H. L. Grubin, and D. K. Ferry, *J. Physique, Colloq. C-10*, **42**, 307 (1981).
- [3] J-R. Zhou and D. K. Ferry, *IEEE Trans. Electron Dev.* **39**, 473, (1992).
- [4] J-R. Zhou and D. K. Ferry, *IEEE Trans. Electron Dev.* **39**, No. 8, (1992).
- [5] T. J. Bordelon, X-L. Wang, C. M. Maziar, And A. F. Tasch, *Sol.State Electron.* **35**, 131 (1992).
- [6] U. Fano, *Rev. Mod. Phys.* **29**, 74 (1957).
- [7] P. Lugli and D. K. Ferry, *IEEE Trans. Electron Dev.* **32**, 2431 (1985).
- [8] M. Kuzuhara, T. Itoh, and Karl Hess, *Sol.-State Electron.* **33**, 1857 (1989).
- [9] T. Shawki, G. Salmer, and O. El-Sayed, *IEEE Trans. Comp.-Added Design.* **9**, 1150 (1990).
- [10] A. M. Krivan, J-R Zhou, and D. K. Ferry, *Physics Lett.* **A138**, 8 (1989).
- [11] J. Hauser, *Sol.-State Electron.* **10**, 577 (1967).